Ontology-Driven Learning of Bayesian Network for Causal Inference and Quality Assurance in Additive Manufacturing

Ruimin Chen, Yan Lu, Paul Witherell, Timothy W. Simpson, Soundar Kumara, and Hui Yang

***Abstract*—Additive manufacturing (AM) enables the creation of complex geometries that are difficult to realize using conventional manufacturing techniques. Advanced sensing is increasingly being used to improve AM processes, and installing different sensors onto AM systems has yielded more data-rich environments. Transforming data into useful information and knowledge (i.e., causality detection and process-structure-property (PSP) relationship identification) is important for achieving the necessary quality assurance and quality control (QA/QC) in AM. However, causality modeling and PSP relationship establishment in AM are still in early stages of development. In this paper, we develop an ontology-based Bayesian network (BN) model to represent causal relationships between AM parameters (i.e., design parameters and process parameters) and QA/QC requirements (e.g., structure properties and mechanical properties). The proposed model enables engineering interpretations and can further advance AM process monitoring and control.**

***Index Terms*—Additive manufacturing, AI-based methods, probabilistic inference.**

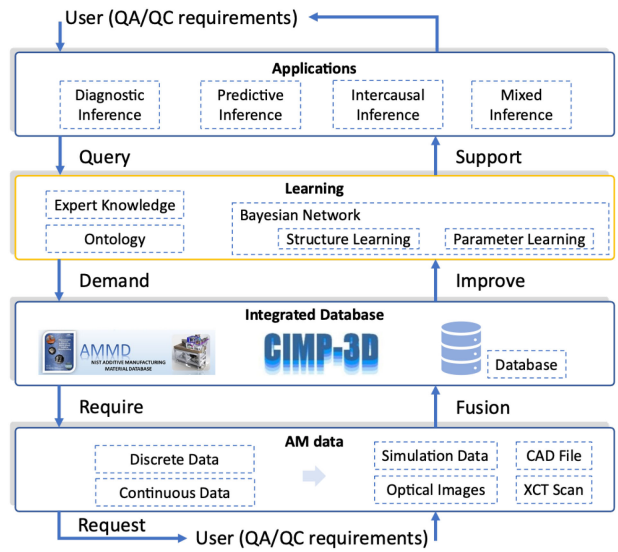

Fig. 1. A four-level framework for AM data management and QA/QC.

I. Introduction

ADVANCED sensing is increasingly integrated into additive manufacturing (AM) to enhance process understanding and improve process control, leading to data-rich environments. A four-level framework for AM data management and quality improvement is shown in Fig. 1 [1]. Sensors capture data related to AM processes and an integrated database stores heterogeneous data from multiple sensors. Predictive models and knowledge are extracted from the collected data to further support process monitoring and quality control. Realizing the full potential of sensing data will lead to an unprecedented opportunity to understand the AM process and offer a new sensor-based solution for quality assurance and quality control (QA/QC). Current practices for QA/QC focus on correlation analysis, which utilizes features (i.e., design parameters, process parameters) to predict the quality of AM builds [2], [3]. A comprehensive review related to QA/QC management of AM is discussed in [4]. However, correlation does not imply causation. New challenges lie in integrating all the information into actionable AM knowledge that captures explicit causal relations, for example, how to select the right parameters to fabricate AM parts that meet QA/QC requirements.

A Bayesian network (BN) contains a graphical structure that represents causal relationships among a large number of variables and allows for probabilistic causal inferences using the observed variables. It moves one step forward to support the inference of causality from observational data and improves interpretability at the same time. Bayesian inference is widely used in early expert system development. The conditional probabilities are used to represent complex relationships by the BNs [5]. Despite numerous computational models are developed to represent AM sub-processes. Identifying causal interconnections between variables becomes a challenging task. While there

Manuscript received February 28, 2021; accepted June 11, 2021. Date of publication June 16, 2021; date of current version June 29, 2021. This letter was recommended for publication by Associate Editor X. Xie and Editor J. Yi upon evaluation of the reviewers' comments. *(Corresponding author: Hui Yang.)*

Ruimin Chen, Soundar Kumara, and Hui Yang are with the Harold and Inge Marcus Department of Industrial and Manufacturing Engineering, The Pennsylvania State University, University Park, PA 16802 USA (e-mail: rxc91@psu.edu; skumara@psu.edu; huy25@psu.edu).

Yan Lu and Paul Witherell are with the National Institute of Standards and Technology, Gaithersburg, MD 20899 USA (e-mail: yanlunj@gmail.com; paul.witherell@nist.gov).

Timothy W. Simpson is with the Harold and Inge Marcus Department of Industrial and Manufacturing Engineering, The Pennsylvania State University, University Park, PA 16801 USA, and also with the Center for Innovative Materials Processing 3D (CIMP-3D), The Pennsylvania State University, University Park, PA 16801 USA (e-mail: timothy.simpson@psu.edu).

Digital Object Identifier 10.1109/LRA.2021.3090020

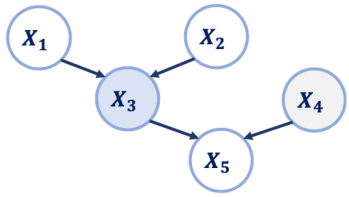

Fig. 2. An example of the Markov condition: given the parents X_1 and X_2, X_3 is conditionally independent of its non-descendant X_4.

have been some notable contributions to the BN structure from automatically-generated observational data [6]–[8], little has been done to integrate BN learning with AM domain knowledge.

In this paper, we develop an ontology-based Bayesian network modeling framework for extracting causal relationships among AM parameters, as a key function for the Learning layer in Fig. 1. BN modeling contains two steps: namely structure learning and parameter learning. The structure of BN represents the qualitative relationships between variables, and parameter values help quantify the interconnections from probability distributions. In this study, we leverage an AM ontology to provide necessary and prior domain knowledge for modeling the causal connections in BN learning. Specifically, we integrate the domain knowledge from our specialized process-based AM ontology with parameter-based data processing and structure learning (i.e., to learn the skeleton of a BN) to create a causal network. Early experimental results demonstrate that our ontology-based BN modeling methodology is capable of extracting important causal relationships on which process control can be predicated.

The rest of the paper is organized as follows: Section II reviews related literature on BN and ontology. Section III presents the experimental setup, quantifier extraction, and the proposed ontology-based BN modeling methodology. Experimental results are provided in Section IV. Section V summarizes this study.

II. Research Background

Bayesian networks, also called Bayesian belief networks or causal probabilistic networks, emerged from probabilistic reasoning in artificial intelligence and has been applied to a wide range of problems, ranging from text analysis [9] to medical diagnosis [10]. A Bayesian network is a directed acyclic graph (DAG) $\mathcal{G}$, in which nodes $\mathbf{V} = \{X_1, X_2 \ldots, X_n\}$ denote the set of random variables of interests and edges $\mathbf{E}$ represent the causal influences among the n variables in $\mathbf{V}$ [5]. As shown in Fig. 2, a BN must satisfy the Markov condition where every variable $X_i \in \mathbf{V}$ is independent of any subset of its non-descendant variables conditioned on the set of its parents Pa_i. Note that the directed edge from Pa_i to X_i indicates a direct causal influence that Pa_i has on X_i.

BN gives a structural means to learn and represent causality which helps in capturing causal relationships in a given domain. Ontology, on the other hand, helps to build the conceptual relationships between various entities in a domain of study. At the lowest level of abstraction, it helps to understand measurable (direct or indirect) variables in a system. In principle, both BN and ontology result in the information, navigation, and analysis of networks. However, little has been done to integrate ontology networks with automated Bayesian learning for AM QA/QC. Li and Shi [11] proposed a causal modeling approach to improve the existing causal discovery algorithm by integrating manufacturing domain knowledge (i.e., rolling processes) with the BN learning. Specifically, they combined domain knowledge with variable selection and variable discretization to reduce the search space. Mokhtarian *et al.* [12] constructed the structure of a BN based on physical relationships between variables. An analytical hierarchy process is utilized to collect preferences from experts. Wang *et al.* [13] proposed a knowledge management system using BN to model AM knowledge in the presence of uncertainty and fill the knowledge gap between designers and AM technologies. Similarly, the BN structure is generated solely from the domain knowledge. Hertlein *et al.* [14] proposed a BN model with four process parameters and five quality characteristics for AM, which is a conditional linear Gaussian BN where nodes can be both discrete and continuous. However, parametric assumptions for mixed data (i.e., continuous and discrete) tend to have practical limitations, as they impose constraints on arcs. For example, a continuous node cannot be the parent of a discrete node. Jing and Ma [15] proposed a fuzzy Bayesian Network to study the AM's adaptiveness. Bacha *et al.* [16] and Verma *et al.* [17] utilized the BN for fault diagnosis, but network structures are assumed to be known in the prior knowledge. In addition, Tran *et al.* [18], [19] investigated the inference of sparse networks from noisy and nonstationary processes, studied the latent connectivity in the sparse network, and further leverage the dynamic network for change detection. In the present paper, we instead focus on the integration of manufacturing ontology networks with BN learning and modeling for AM QA/QC.

While BNs are graphical structures for representing the probabilistic relationships among variables and doing probabilistic inference with those variables, ontology describes domain concepts and their semantic relationships that can represent causality. Our previous work developed ontology models to support AM process model development and reuse [20], [21]. The AM process ontology captures a network of variables that can be visualized in a graph, and allows users to navigate complex relationships and understand the connections between different process parameters, microstructural characteristics, and mechanical properties of AM parts. Ontology shows strong potential to support the construction of Bayesian networks [22]. However, most of the existing works focus on utilizing ontology to select variables, identify relationships, and assign conditional probability distributions. Little has been reported on how to integrate ontological representation with automated BN learning algorithms. At the same time, automated BN structure and parameter learning from data are often insufficient in practice due to the limited availability of data. In this study, we utilize AM ontology to extract the causal connections among variables.

III. Methodology

This paper presents an ontology-driven Bayesian network modeling for AM design-process-structure-property causal

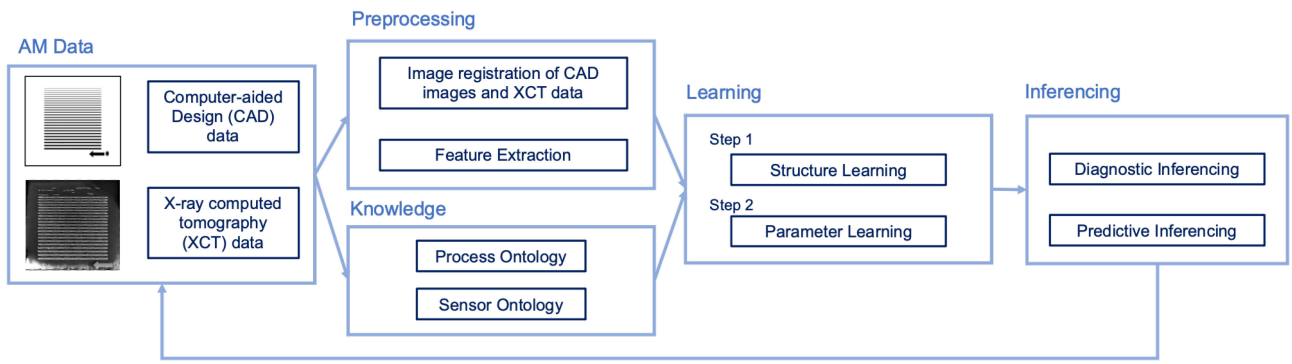

Fig. 3. The flow chart of the proposed research methodology.

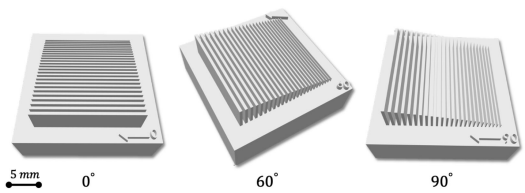

Fig. 4. Thin-wall parts fabricated with three orientations with respect to the travel direction of recoater blade (i.e., indicated by the arrow on each part).

analysis on which future process control analytical methods can be developed. As shown in Fig. 3, the modeling procedure has four steps. First, we obtain pre-processing computer-aided design (CAD) slices and post-processing X-ray computed tomography (XCT) data. Then, we register the data and extract important features from them. Next, by integrating AM ontology, we perform hybrid structure learning (i.e., combining the conventional score-based algorithms and constraint-based algorithms) to study the causal relationships between the features. Note that the BN modeling is performed in an inherently Bayesian fashion. Finally, we perform predictive inference and diagnostic inference to navigate on the constructed BN.

A. *Offline Quantification of Build Quality Using Layer-Wise XCT Scan Images*

In this experiment, thin-wall parts were built with the powder bed fusion (PBF) technology from Spherical ASTM B348 Grade 23 Ti-6Al-4 V powder with a size distribution of 14-45 μm on an EOS M280 machine. PBF refers to a family of AM processes in which thermal energy selectively fuses regions of a powder bed [23]. During the PBF fabrication, a layer of metal powder is first spread across a build plate, then a certain area is selectively melted (fused) with an energy source, such as an electron beam. This procedure continues until the top layer of the build is fused.

As shown in Fig. 4, thin-wall builds are fabricated in three orientations (i.e., 0°, 60°, and 90°) with respect to the travel direction of the recoater blade (i.e., indicated by the arrow on each part). Standard EOS M280 processing parameters for 60-μm layers were used in the experiments, i.e., the laser power and velocity settings are 340 W and 1250 mm/s, respectively. Each build consists of 25 thin-walls with a height/width ratio of 10. The width of thin-walls increases from 0.06 mm, with a step size

TABLE I
THE VARIATIONS IN CONTOUR SPACES WITHIN CONTOUR FROM THIN-WALL 1 TO THIN-WALL 25

Thin-wall Number	W_h mm	Thin-wall Number	W_h mm	Thin-wall Number	W_h mm	Thin-wall Number	W_h mm	Thin-wall Number	W_h mm
1	0.244	6	0.190	11	0.142	16	0.092	21	0.045
2	0.234	7	0.183	12	0.136	17	0.082	22	0.033
3	0.220	8	0.167	13	0.125	18	0.076	23	0.022
4	0.208	9	0.159	14	0.114	19	0.059	24	0.011
5	0.198	10	0.154	15	0.102	20	0.049	25	N/A

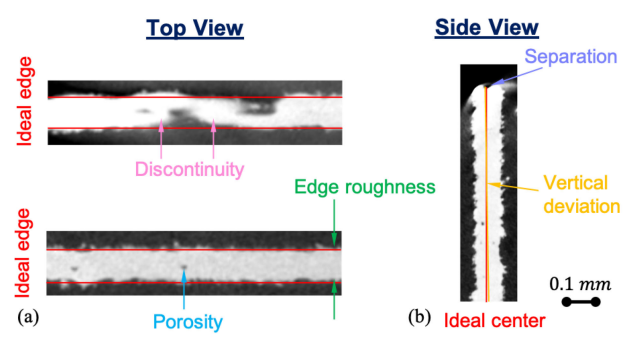

Fig. 5. (a) Top view of the XCT slice in the thin-wall 5 at layer 70 of 0° build, with quality issues such as edge roughness, discontinuity, and porosity; (b) side view of the XCT slice in the thin-wall 5 at layer 70 of 0° build, with quality issues such as separation and vertical deviation.

of 0.01 mm, to 0.3 mm. Information related to contour space is summarized in Table I. Note that contour space is defined as the width between inner contours in each thin-wall, and there is a 67-degree rotation for the hatching paths on each layer by the default setting of the EOS 280 machine.

Post build XCT data are obtained on a General Electric V | tome|X system with a voxel size of 14 μm^3. XCT slices are obtained through the volume graphics viewer myVGL. Several defects can be seen from XCT slices after image registration. For the detailed information related to registration, please refer to our previous work in [24]. As shown in Fig. 5 (a), we can detect discontinuity, edge variation, and porosity from the top view. In addition, we can observe vertical deviation as well as separation on the top of each thin-wall. Note that larger defects run down the center of thin-walls according to Fig. 5 (b). The following features are extracted from the XCT scan to quantify the quality of fabricated parts.

- **Edge roughness:** this feature measures how much the printed edge deviates from the CAD design. For example,

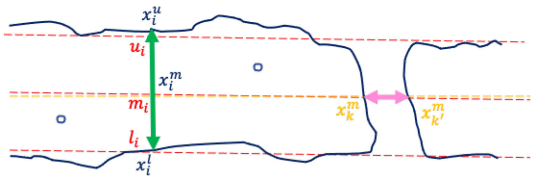

Fig. 6. Feature extraction from thin-walls from XCT slices.

the edge roughness of the upper edge in Figure. 6 is calculated as:

$$\sigma_e = \sqrt{\frac{\sum_{i=1}^{N}(x_i^u - u_i)^2}{N}} \tag{1}$$

where x_i^u is the ith pixel in the upper printed edge, u_i is the ith pixel in the upper CAD edge, and N is the total length of the thin-wall.

- **Thickness:** the thickness $\bar{t}$ of each thin-wall is calculated as:

$$\bar{t} = \frac{\Sigma_{i=1}^{N}||x_i^u - x_i^l||}{N} \tag{2}$$

where x_i^l is the ith pixel in the lower printed edge.

- **Vertical deviation:** this feature quantifies how far the center of each thin-wall deviates from the designed center.

$$\bar{v} = \frac{\Sigma_{i=1}^{N}(x_i^m - m_i)}{N} \tag{3}$$

where m_i is the middle point of x_i^u and x_i^l.

- **Discontinuity:** discontinuity is calculated as the length between two pixels on the centerline of the border.

$$d = ||x^{m_k} - x^{m'_k}|| \tag{4}$$

where x^{m_k} and $x^{m'_k}$ are the kth and k'^{th} pixel in m_i, respectively.

- **Number of pores:** this feature counts the number of pores in each layer of the thin-wall. The number of 8-connected binarized XCT pixels over a layer translates to the pore count [25].
- **Density:** this feature is represented by

$$\rho = \frac{\Sigma_{i=1}^{N}\Sigma_{j=1}^{M}I(i,j)}{NM} \tag{5}$$

where $I(i,j)$ is the intensity value of the binarized XCT pixel.

B. Learning a Bayesian Network From Data

As shown in Fig. 3, BN modeling can be performed with two steps in an inherently Bayesian fashion:

$$P(\mathcal{G}, \Theta|\mathbf{V}) = P(\mathcal{G}|\mathbf{V}) \cdot P(\Theta|\mathcal{G}, \mathbf{V}) \tag{6}$$

where $\mathcal{G}$ denotes the structure of the DAG, and Θ represents parameters of the BN given the $\mathcal{G}$ obtained from structure learning. $\mathbf{V}$ is the observational data.

Three types of algorithms are commonly utilized to learn the structure of BNs from the observational data: namely constraint-based algorithms, score-based algorithms, and hybrid algorithms. While constraint-based algorithms (e.g., PC [6]) are based on causal graphical models by Verma and Pearl [17], score-based algorithms (e.g., Greedy Equivalent Search [26]) are general-purpose optimisation techniques for structure learning. Specifically, constraint-based methods leverage conditional independence tests to construct the oriented graph, and score-based algorithms maximize the goodness-of-fit scores of the DAG structure. Hybrid algorithms (e.g., Max-Min Hill-Climbing [7]) first construct the skeleton of a DAG, and then utilize score-based functions to determine the orientation of edges, which combine the advantages from two approaches. In this paper, we integrate the hybrid learning algorithm (i.e., H2PC [27]) with the ontology graph to identify the causal relations between variables in AM. Specifically, the domain knowledge of AM ontology is incorporated into the following steps: (1) discretization of continuous data, and (2) adding constraints between variables from the ontology graph.

Algorithm 1: The Proposed Ontology-based Structure Learning for Bayesian Network.

Input: a variable set $\mathbf{V}$, an empty DAG $\mathcal{G}$
1: discretize each continuous variable $X_i \in \mathbf{V}$
2: $\mathcal{G}_o \leftarrow$ ontology graph
3: $\mathbf{PC} \leftarrow HPC(\mathbf{V}, \mathcal{G}_o)$ // identify the parents and children set of each variable through HPC algorithm
4: **For** each pair of $(X_1, X_2) \in \mathbf{PC}$:
5: $\mathcal{G} \leftarrow HC(\mathbf{PC}, \mathcal{G}, \mathcal{G}_o)$ // begins with an empty graph, add, delete, remove edge that leads to the largest increase in score from greedy hill-climbing search
Output: DAG $\mathcal{G}$

The H2PC algorithm learns the BN in two steps. First, it constructs the structure or the skeleton of BN through the constraint-based algorithm. Then, it performs a Bayesian scoring greedy search to add, delete, and change the direction of the edges. In the proposed Algorithm 1, we integrate the ontology information (i.e., $\mathcal{G}_0$) into several steps of HPC and H2PC algorithms. In the first step, the HPC algorithm combines the advantages of incremental and divide-and-conquer methods, targets for the parent-children discovery and contains three sub-algorithms, namely Data-Efficient Parents and Children Superset (DE-PCS), Data-Efficient Spouses Superset (DE-SPS), and Incremental Association Parents and Children with false discovery rate control (FDR-IAPC), respectively. Specifically, DE-PCS and DE-SPS search for supersets of parent, children, and spouses of nodes. In the second step, the H2PC performs a greedy hill-climbing search in the space of BN. The search starts with an empty graph and further adds, deletes, or reverses the edge direction that increase the score. Note that the search only adds the edges that are obtained in the previous step, which is the key difference between the greedy hill-climbing search in the H2PC algorithm and the direct utilization of greedy search to learn a BN structure. As shown in Algorithm 1, we first search the parent-children sets $\mathbf{PC}$ for every node in the network through HPC. Then, for all pairs of $(X_i, X_j) \in \mathbf{V}$, add X_i in $\mathbf{PC}_{X_j}$ and add X_j in $\mathbf{PC}_{X_i}$ if

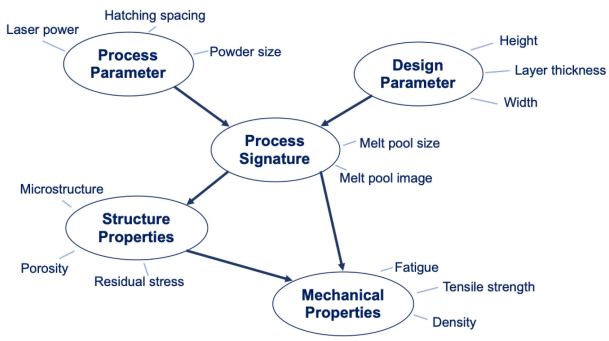

Fig. 7. The visualization of an AM ontology graph.

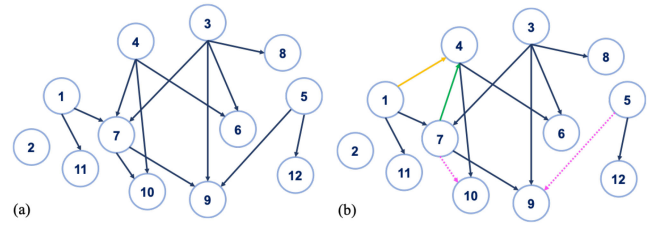

Fig. 8. (a) The constructed BN with knowledge from AM ontology; (b) the constructed BN without knowledge from AM ontology. Dashed arrows in pink shows edges that are not learned, solid yellow arrows indicate the edges that are not supposed to be learned, solid green arrows denote edges learned in the wrong direction.

TABLE II
PROCESS VARIABLES AND QUALITY VARIABLES

Variable	Code	Node	Type
Input variable	1	Contour Space	Process Parameter
	2	Scan Path	Process Parameter
	3	Orientation	Design Parameter
	4	Width	Design Parameter
	5	Height	Design Parameter
QA/QC output	6	Edge Roughness	Structure Proprieties
	7	Thickness	Structure Proprieties
	8	Vertical deviation	Structure Proprieties
	9	Discontinuity	Structure Proprieties
	10	Number of Pores	Structure Proprieties
	11	Fin Separation	Structure Proprieties
	12	Density	Mechanical Proprieties

$X_i \in HPC(X_j)$ and $X_j \in HPC(X_i)$. Next, starting from an empty graph, we only perform the operator add edge $X_i \rightarrow X_j$ if $X_j \in \mathbf{PC}_{X_i}$.

IV. EXPERIMENTAL RESULTS

In this section, we evaluate and validate the proposed ontology-based BN modeling methodology with real-world data and then benchmark the performance of obtained BN models with and without AM ontology. As shown in Fig. 7, data obtained from AM processes can be classified into five categories, namely process parameter, design parameter, process signature, structured properties, and mechanical properties. In the ontology graph, process signatures can cause variations in structural properties and mechanical properties, process parameter can also lead to changes in process signature. However, BN obtained structural properties and mechanical properties cannot cause either process parameters or process signature. Note that there are important temporal relationships between variables. For example, the shapes of melt pools can be different due to variations in the recoating orientation (e.g., tails caused by the travel direction of the laser). Low laser power can cause porosity in the part, and further impact the mechanical properties (e.g., tensile strength) of the final product. Causal connections show that process related parameters influence the mechanical and structural properties.

As mentioned in Section III-A, we extract a total of 12 variables from different parameter groups (see Table II). We discretize features based on domain knowledge as described below. Note that each level of the feature should contain a similar number of observations to avoid bias.

- **Contour space:** is the measured width between the hatches of the inner rectangle for each thin-wall. We discretize the contour space into three groups based on the melt pool diameter (i.e. 110 μm) and laser diameter (i.e. 80 μm).
- **Scan path:** there is a 67-degree rotation for the hatching paths on each layer by the default setting of the EOS 280 machine. Therefore, the scan path is batched into three groups.
- **Orientation:** orientation has three levels because three parts are built under three directions (i.e., 0°, 60°, 90°).
- **Width:** width is divided into four balanced groups.
- **Height:** height is grouped into four levels according to the height/width ratio of each layer. For example, if the height/width ratio of a layer is 10, and the width of the thin-wall is 0.3 mm, then the height is 3.0 mm.
- **Edge roughness:** edge roughness has three levels according to warning limits of the distribution.
- **Thickness:** thickness is partitioned into three groups, i.e., within 10% tolerance, above 10% tolerance, and below 10% tolerance.
- **Vertical deviation:** binary variable which indicates the direction of deviation, i.e., deviates towards left or right.
- **Discontinuity:** discontinuity is divided into three groups where each group consists of a similar number of data.
- **Number of pores:** this feature counts the number of pore with a diameter greater than 100 μm [28].
- **Separation:** binary variable where $X_{11} = L1$ stands for there is a separation of the top of the fin, and $X_{11} = L2$ denotes there is no separation.
- **Density:** in our experiment, we set $X_{12} = L1$ when the density of the thin-wall is greater than or equal to 95%, and $X_{12} = L2$ when is less than 95% [29].

We separate 80% of our data for training and 20% for testing in our analysis. For the construction of BN, we performed the model averaging for the structure learning. Note that structures were slightly different among each of the 50 runs. Therefore, we kept arcs that are learned for more than 80% of the time. Figure. 8 compares two BN structures learned with and without AM ontology. Note that the dashed arrows in pink show edges that are not learned, solid yellow arrows indicate the edges that are not supposed to be learned, solid green arrows denote edges

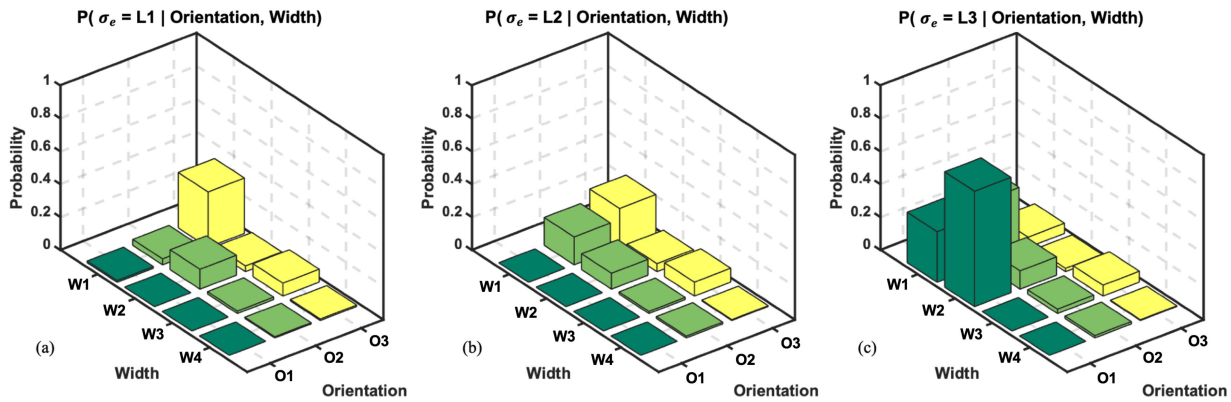

Fig. 9. (a) Conditional distribution plots of $\sigma_e = L1$ given orientation and width at different levels, (b) conditional distribution plots of $\sigma_e = L2$ given orientation and width at different levels, and (c) conditional distribution plots of $\sigma_e = L3$ given orientation and width at different levels.

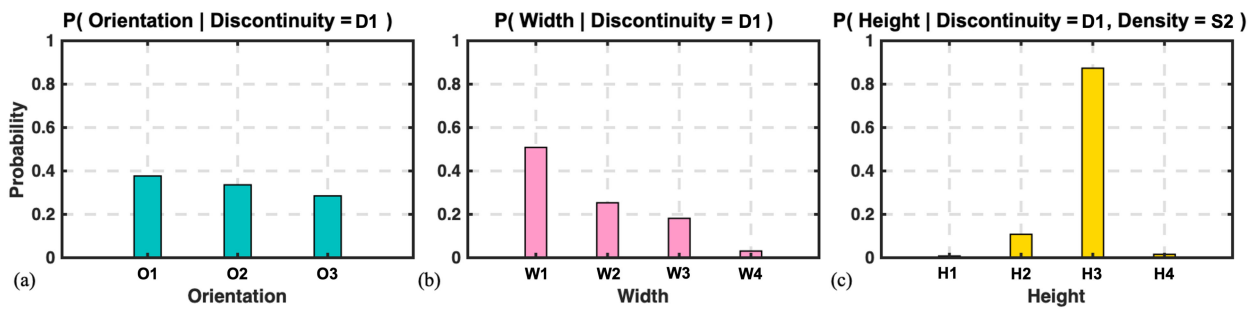

Fig. 10. (a) Conditional distribution plots of orientation at different levels given discontinuity $= D1$, (b) conditional distribution plots of width at different levels given discontinuity $= D1$, and (c) conditional distribution plots of height at different levels given discontinuity $= D1$ and density $= S2$.

learned in the wrong direction. In Figure. 8 (b), the contour space is linked to width, showing that there is a causal relationship between the two nodes. However, design parameters cannot be causal factors of process parameters according to the ontology knowledge, and vice versa. In addition, the structure indicates that thickness is the causal factor of width, structure properties if not the causal factor of design parameters based on the temporal relationships between nodes in the ontology graph. In addition, some of the edges (i.e., two arcs in pink) cannot be learned without domain knowledge.

As shown in Fig. 8 (a), the causal relationships among variables can be identified qualitatively through the learned structure, and quantitatively through predictive inference and diagnostic inference. Note that we predict from cause to effect, and we diagnosis from effect to cause. For example, $P(\sigma_e|\text{orientation, width})$ can be obtained by conditional distribution plots in Fig. 9. Note that orientation (node 1) has three levels, width (node 4) has four levels, and the edge roughness (i.e., σ_e) has three levels. Based on the results of predictive inference, it is more likely to have a higher probability of severe edge roughness (i.e., $\sigma_e = L3$ when thin-walls have a width of $L2$ (i.e., $(0.16\,\text{mm}, 0.21\text{mm}]$) and orientation $L1$ (i.e., $0°$). Further, we obtained the prediction accuracy through 20% testing dataset. For example, the prediction accuracy for thin-wall LWR, thickness, and density are $78.70\% \pm 0.012$, $87.77\% \pm 0.011$, and $96.79\% \pm 0.005$, respectively. The proposed ontology-driven BN modeling helps integrate the AM engineering knowledge with network learning to discover causal relationships among variables. As a result, BN results can be utilized by AM engineers and technicians for backward diagnosis and the interpretation of causal relationships in PBF AM processes.

The example of diagnostic inference is shown in Fig. 10. Fig. 8(a) shows that contour space, width, orientation, and height are causal factors of the discontinuity. Therefore, we can determine which state of these causal factors has the least probability to cause the discontinuity issue in the thin-wall builds. For example, when discontinuity is $D1$ (i.e., no discontinuity), we should build the part under orientation $O1$ with width in the range of $W2$ according to Fig. 10 (a) and (b), respectively. In addition, height is the causal factor of both density and discontinuity, so we can perform the diagnostic inference for $P(\text{height}|\text{discontinuity, density})$. In Fig. 10 (c), when the height of the thin-wall is at $H3$ (i.e., height/width ratio is in (5, 7.5]), the part has better quality because the discontinuity is at $D1$ (i.e., no discontinuity) and density is at $S2$ (i.e., density is greater than 95%).

V. Discussions and Conclusions

With the rapid development of sensing capabilities, a variety of sensors are being installed on different AM systems to collect data, increase performing visibility, as well as to improve the QA/QC of AM builds. The challenge now lies in integrating all the data and information into useful AM knowledge, and making this process more repeatable and reliable.

In this paper, we propose an ontology-based BN model for the representation of causal relationships between AM parameters (i.e., design parameters and process parameters) and QA/QC requirements (e.g., structure properties and mechanical properties). We leverage the real-world data from thin-walls to demonstrate the prediction inference and diagnostic inference from the constructed BN model. The proposed methodology facilitates both forward prediction and backward diagnosis. We illustrated two quantitative results for predicting the quality as well as root cause diagnosis with two examples, respectively. In addition, we compared experimental results between BN learning methods with and without AM ontology. The proposed methodology enables engineering interpretations of causality interrelations in AM and can further facilitate AM process monitoring and control. Although BN learned is aimed at the PBF AM process in this work, the proposed ontology-based BN modeling methodology can be further extended and generalized to other AM processes. However, because there are variations in process parameters and materials in different AM processes, it is necessary to incorporate newly added domain knowledge (i.e., ontology networks) and introduce more nodes (e.g., material, design variables, process parameters, sensors) in the model generalization. The proposed algorithm may also need slight modifications for different data types, but the structure and parameter learning process is generally applicable. Future work will continue to investigate the dynamics between empirical observations and their physical counterparts, with the goal of a methodology that does not "ground" one with the other but instead supports reciprocated learning in the identification of key variables and causal relationships.

Acknowledgment

The authors would like to thank the National Institute of Standards and Technology (NIST) for supporting this work. We gratefully acknowledge the CIMP-3D at Penn State University for providing the data utilized in this research, in particular Corey Dickman for designing and executing the test builds, Griffin Jones for performing the CT scans, and students Gabi Gundermann and Matt Dolack for their preliminary analysis.

References

[1] Y. Lu, Z. Yang, D. Eddy, and S. Krishnamurty, "Self-improving additive manufacturing knowledge management," in *Proc. Int. Des. Eng. Tech. Conf. Comput. Informat. Eng. Conf.*, vol. 51739. American Society of Mechanical Engineers, 20 18, Art. no. V01BT02A016.

[2] R. Chen, F. Imani, E. Reutzel, and H. Yang, "From design complexity to build quality in additive manufacturing-a sensor-based perspective," *IEEE Sensors Lett.*, vol. 3, no. 1, pp. 1–4, Jan. 2018, Art no. 7101904.

[3] B. Yao, F. Imani, A. S. Sakpal, E. Reutzel, and H. Yang, "Multifractal analysis of image profiles for the characterization and detection of defects in additive manufacturing," *J. Manuf. Sci. Eng.*, vol. 140, no. 3, 2018.

[4] H. Yang *et al.*, "Six-sigma quality management of additive manufacturing," *Proc. IEEE*, vol. 109, no. 4, pp. 347–376, Apr. 2021.

[5] J. Pearl, "Graphical models for probabilistic and causal reasoning," *Quantified Representation Uncertainty Imprecision*, pp. 367–389, 1998.

[6] D. Colombo and M. H. Maathuis, "Order-independent constraint-based causal structure learning," *J. Mach. Learn. Res.*, vol. 15, no. 1, pp. 3741–3782, 2014.

[7] I. Tsamardinos, L. E. Brown, and C. F. Aliferis, "The max-min hill-climbing bayesian network structure learning algorithm," *Mach. Learn.*, vol. 65, no. 1, pp. 31–78, 2006.

[8] M. Scutari, C. E. Graafland, and J. M. Gutiérrez, "Who learns better bayesian network structures: Accuracy and speed of structure learning algorithms," *Int. J. Approx. Reasoning*, vol. 115, pp. 235–253, 2019.

[9] A. Dong and A. M. Agogino, "Text analysis for constructing design representations," *Artif. Intell. Eng.*, vol. 11, no. 2, pp. 65–75, 1997.

[10] M. B. Sesen, A. E. Nicholson, R. Banares-Alcantara, T. Kadir, and M. Brady, "Bayesian networks for clinical decision support in lung cancer care," *PLoS one*, vol. 8, no. 12, p. e 82349, 2013.

[11] J. Li and J. Shi, "Knowledge discovery from observational data for process control using causal bayesian networks," *IIE Trans.*, vol. 39, no. 6, pp. 681–690, 2007.

[12] H. Mokhtarian, A. Hamedi, H. P. Nagarajan, S. Panicker, E. Coatanéa, and K. Haapala, "Probabilistic modelling of defects in additive manufacturing: A case study in powder bed fusion technology," *Procedia CIRP*, vol. 81, pp. 956–961, 2019.

[13] Y. Wang, R. Blache, P. Zheng, and X. Xu, "A knowledge management system to support design for additive manufacturing using bayesian networks," *J. Mech. Des.*, vol. 140, no. 5, pp. 051701-1–13, 2018.

[14] N. Hertlein, S. Deshpande, V. Venugopal, M. Kumar, and S. Anand, "Prediction of selective laser melting part quality using hybrid bayesian network," *Additive Manuf.*, vol. 32, 2020, Art. no. 101089.

[15] L. Jing and J. Ma, "Additive manufacturing adaptiveness analysis using fuzzy bayesian network," in *Proc. Int. Des. Eng. Tech. Conf. Comput. Informat. Eng. Conf.*, vol. 83952. American Society of Mechanical Engineers, 2020, Art. no.. V00 6T06A004.

[16] A. Bacha, A. H. Sabry, and J. Benhra, "Fault diagnosis in the field of additive manufacturing (3 d printing) using bayesian networks." *Int. J. Online Biomed. Eng.*, vol. 15, no. 3, pp. 110–123, 2019.

[17] T. Verma and J. Pearl, Equivalence and synthesis of causal models. UCLA, Computer Science Department, 1991.

[18] H. M. Tran and S. T. Bukkapatnam, "Inferring sparse networks for noisy transient processes," *Sci. Rep.*, vol. 6, no. 1, pp. 1–13, 2016.

[19] H. M. Tran, S. T. Bukkapatnam, and M. Garg, "Detecting changes in transient complex systems via dynamic network inference," *IISE Trans.*, vol. 51, no. 3, pp. 337–353, 2019.

[20] B.-M. Roh, S. R. Kumara, T. W. Simpson, P. Michaleris, P. Witherell, and I. Assouroko, "Ontology-based laser and thermal metamodels for metal-based additive manufacturing," in *Proc. Int. Des. Eng. Tech. Conf. Comput. Informat. Eng. Conf.*, vol. 50077. American Society of Mechanical Engineers, 2016, Art. no. V01AT02A043.

[21] P. Witherell *et al.*, "Toward metamodels for composable and reusable additive manufacturing process models," *J. Manuf. Sci. Eng.*, vol. 136, no. 6, pp. 061025-1–9, 2014.

[22] S. Fenz, "An ontology-based approach for constructing bayesian networks," *Data Knowl. Eng.*, vol. 73, pp. 73–88, 2012.

[23] *ASTM*, Standard terminology for additive manufacturing technologies. ASTM International, West Conshohocken, PA, Standard No ASTM 52900-15., 2012.

[24] R. Chen, P. Rao, Y. Lu, E. Reutzel, and H. Yang, "Recurrence network analysis of design-quality interactions in additive manufacturing," Additive Manuf., vol. 39, 2021, Art. no. 101861.

[25] F. Imani, A. Gaikwad, M. Montazeri, P. Rao, H. Yang, and E. Reutzel, "Process mapping and in-process monitoring of porosity in laser powder bed fusion using layerwise optical imaging," *J. Manuf. Sci. Eng.*, vol. 140, no. 10, pp. 101009-1–14, 2018.

[26] D. M. Chickering, "Optimal structure identification with greedy search," *J. Mach. Learn. Res.*, vol. 3, pp. 507–554, 2002.

[27] M. Gasse, A. Aussem, and H. Elghazel, "A hybrid algorithm for bayesian network structure learning with application to multi-label learning," *Expert Syst. Appl.*, vol. 41, no. 15, pp. 6755–6772, 2014.

[28] R. Snell *et al.*, "Methods for rapid pore classification in metal additive manufacturing," *JOM*, vol. 72, no. 1, pp. 101–109, 2020.

[29] A. J. Dunbar, G. J. Gunderman, M. C. Mader, and E. W. Reutzel, "Fabrication and quality assessment of thin fins built using metal powder bed fusion additive manufacturing," in *Proc. 28th Annu. Int. Solid Freeform Fabr. Symp.-An Additive Manuf. Conf.*, SFF 2017, 2020, pp. 2650–2663.